K. Tanabe, H. Kubota, A. Sai and N. Matsumoto, "Data selection and de-noising based on reliability for long-range and high-pixel resolution LiDAR," 2018 IEEE Symposium in Low-Power and High-Speed Chips (COOL CHIPS), Yokohama, 2018, pp. 1-3. doi: 10.1109/CoolChips.2018.8373079

Data Selection and De-noising Based on Reliability for Long-Range and High-Pixel Resolution LiDAR

Ken Tanabe, Hiroshi Kubota, Akihide Sai and Nobu Matsumoto
Toshiba Electronic Devices & Storage Corporation
580-1, Horikawa-Cho, Saiwai-ku, Kawasaki, Japan
Tel +81-44-548-2522, kenn.tanabe@toshiba.co.jp

Although the Smart Accumulation Technique (SAT) [1] is an optimal averaging algorithm for realizing a long-range and high-pixel-resolution LiDAR system, its maximum effect is guaranteed by de-noising which is quite challenging due to the "range-value-clustering" problem peculiar to SAT. We propose a new algorithm that performs de-noising based on "reliability" provided by accumulating luminous intensities within a cluster. The simulation and measurement results show that the algorithm eliminates the clustering influence, and improves the maximum measurable range by about 2x on 99% of de-noised results, compared with the conventional approach. The overhead of the hardware implementation is small, 1% or less, in regard to Si area and power consumption. (Keywords: LiDAR, de-noising, reliability, cluster, spatial relation, intensity information, background light information, and averaging)

LiDAR systems uniting long-range distance measurement and high-pixel resolution are required to make possible safe and reliable self-driving. Although an averaging algorithm using multiple pixel data improves the S/N ratio equivalently and enables long-range measurement, it degrades pixel resolution when multiple objects exist within the averaging scope. SAT is a "smart accumulation" algorithm which recognizes and selectively averages only the target reflection data by using intensity and background light information. The measurement result demonstrates that SAT enables 200m-range imaging at high-resolution under low S/N conditions [1]. We have developed a power-efficient IC which contains 20ch of SAT circuits, TIAs, ADCs, and TDCs and whose power consumption is 1.7W or less (25°C, typ.). We then demonstrated measurement capability with a LiDAR system embedding the IC from the viewpoint of circuit implementation.

In general, the averaging algorithm needs data selection and de-noising as post-processing because it generates multiple data returns including false data related to random noise, which can be observed when no object exists within measurable distance. However, SAT has a side effect of causing range-value clustering, which makes de-noising difficult without discarding true signals. Without averaging, false range results originating from random noise become isolated outlying data, as shown in Fig.1 (a). In that case, de-noise is possible simply by removing the outlying data (Fig.1 (b)). But when SAT is applied, clustering occurs owing to averaging with random noise, which prevents the random noise from appearing as outlying data, as shown in Fig.1 (c). If no de-noise solution for treating the clustering were available, SAT would not be applicable due to possible misrecognition caused by the false data.

Among existing techniques for de-noising range images, thresholding low intensity (amplitude) values is well-known [2]. Discarding 1st-photon response [3] is a similar approach since it also considers intensity only. But de-noise methods based on intensity often remove true-signal data of low intensity. Using a tri-lateral filter which considers intensity, range, and spatial relation is also proposed [4] [5]. However, tri-lateral filters do not eliminate noise data and have a risk of creating non-existent data. This does not fit the automotive application of LiDAR in which reliability is primarily important. Many efforts have been made using flying pixels [6], but they have not taken the clustering problem into account. While attempts using DNN which inputs peak intensity as reliability have been reported [7], the area/power penalty of DNN should be too large if it is to serve de-noising purposes only. So far, no study has been published which addresses clustering problems and provides a solution that eliminates false data.

In this paper, an algorithm suited for hardware implementation is proposed to select or reject a range value from multiple returns according to reliability provided by accumulating intensity within a cluster. The algorithm never creates non-existent data because it only performs selection or rejection. Furthermore, it can be adapted to real-time applications such as obstacle detection since it supports high-speed hardware implementation.

The newly defined reliability, a key concept of the algorithm, is here presented using the case of a single return per pixel to simplify the explanation. Straightforward extension to multiple returns provides data

selection capability. A cluster of pixels i is defined as a set of neighboring pixels j whose range value is close to that of pixel i, as shown in Fig. 2. Here, a neighbor means pixels within a scope of accumulation. Fig.3 shows the relation of intensity L and cluster size N with various simulated range images, assuming the accumulation scope is sufficiently large. This figure has four thin lines corresponding to relations in cases where the success rates are 0%, 70%, 80%, and 90%. "Success rate 0%" means that no object is detected at the pixel level, as in the sky area. Since lines move toward the upper right as the success rate increases, reliability should become higher with an increase of intensity or cluster size. The bold line indicates a line of $L^2 \times N \approx$const, whose tendency roughly represents simulated relations. Thus, considering $\sqrt{const}$ as the first definition of reliability $R1_i$, in terms of intensity L_i (average intensity / accumulation size) and range D_i and accumulation scope A, $R1_i$ is given by

$$R1_i = L_i \times \sqrt{N_i}, N_i = \sum_{j \in A} p(i,j), p(i,j) = \begin{cases} 1, & |D_j - D_i| \le k \\ 0, & |D_j - D_i| > k \end{cases} \quad (1)$$

The second definition $R2_i$ is given by accumulating ${L_i}^2$ with a cluster instead of ${L_i}^2 \times N_i$ in (1)

$$R2_i = \left[\sum_{j \in A} L_j^2 \times p(i,j)\right]^{\frac{1}{2}}, \; p(i,j) = \begin{cases} 1, & |D_j - D_i| \le k \\ 0, & |D_j - D_i| > k \end{cases} \quad (2)$$

As a reference, we also consider the conventional reliability $R0_i = L_i$ without averaging.

The new reliability definition makes the threshold independent of strength of averaging, *i.e.*, size of accumulation scope, as explained below. Fig. 4 shows the relation of reliability and failure rates on de-noising in the sky area (0% success rate) with the changing size of accumulation scope. Here, black lines at the 1% failure rate indicate thresholds for the reliability of 99% de-noising. As shown in Fig.4, the threshold for R1 and R2, unlike that of R0, is uniquely determined with no dependence on the size of accumulation scope. Note that R1 and R2, by definition, are equal to R0 when the size of accumulation scope is 1. This means that R1 and R2 incorporate the influence of clustering and represent certainty of range data under averaging.

Fig.5 (a) shows success rate vs distance with 99% de-noised results based on optical and electric simulation. Assuming that 90% success rates are criteria for measurable distance, the measurable distance with the proposed reliability is approximately doubled compared to the conventional R0. Fig.5 (b) shows the success rate after 99% de-noising when there was 90% success rate before de-noising. As shown in Fig.5 (b), the success rate with R2 is better than with R1 by 10% or less and is much better than with R0. Furthermore, degradation owing to 99% de-noising can be almost completely suppressed by using the second return with a combination of R2. In Fig.6 and Fig.7, (a) and (b) show the range images captured by the LiDAR with the conventional R0 and the proposed R2 de-noising, respectively. Compared to R0, the proposed method clearly detects an object like a surface of road and a car at a greater distance. A 20ch circuit realizing the algorithm has 113 K gates with power consumption of 15.8mW in 28nm CMOS, which is 1% or less of the AFE and SAT circuits.

[1] K. Yoshioka, H. Kubota, T. Fukushima, S. Kondo, T. T. Ta, H. Okuni, et al., "A 20ch TDC/ADC Hybrid SoC for 240x96-pixel 10%-Reflection <0.125%-Precision 200m-Range-Imaging LiDAR with Smart Accumulation Technique", ISSCC Dig. Tech. Papers, pp.92-93, Feb. 2018.

[2] S. May , D. Droeschel , D. Holz , C. Wiesen , S. Fuchs , I. Overview, "3D Pose Estimation and Mapping with Time-of-Flight Cameras", In IROS Workshop on 3D Mapping, 2008.

[3] C. Niclass, M. Soga, H. Matsubara, M. Ogawa, M. Kagami, "A 0.18um CMOS SoC for a 100m-Range 10fps 200x96 Pixel Time-of-Flight Depth Sensor", ISSCC Dig. Tech. Papers, pp.488-489, 2013.

[4] S. Oishi, R. Kurazume, Y. Iwashita, T. Hasegawa, "Denoising of Range Images using Trilateral Filter and Belief Propagation", Intelligent Robots and Systems, pp.2020-2027, 2011.

[5] P. Choudhury, J. Tumblin, "The trilateral filter for high contrast images and meshes", In Euro-graphics Symposium on Rendering, pp.1-11, 2003.

[6] M. Reynolds, J. Doboš, L. Peel, T. Weyrich, G. Brostow, "Capturing time-of-flight data with confidence". In Computer Vision and Pattern Recognition, 2011. CVPR 2011. IEEE Conference on, pages 945-952. IEEE, 2011.

[7] S. Ito, S. Hiratsuka, M. Ohta, H. Matsubara, M. Ogawa, "Small Imaging Depth LIDAR and DCNN-Based Localization for Automated Guided Vehicle", Sensors 2018, 18, 177.

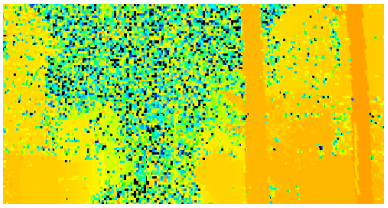

(a) Outputs without averaging

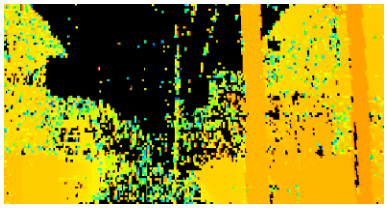

(b) Noise reduction result of (a)

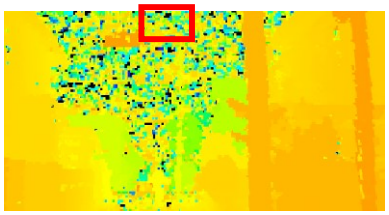

(c) Output with SAT and clustering

(d) Magnified view of (c)

Fig.1 Example of range image

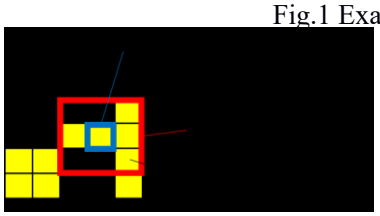

Fig.2 Cluster

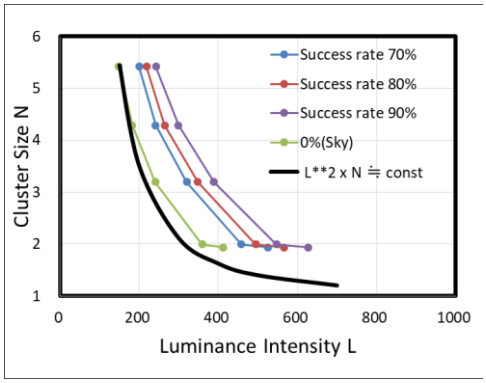

Fig.3. Relation of intensity and cluster size

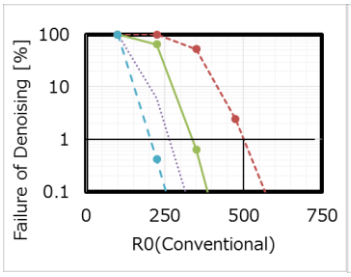

(a) R0 (conventional)

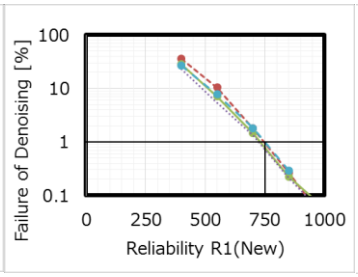

(b) R1 (proposed method 1)

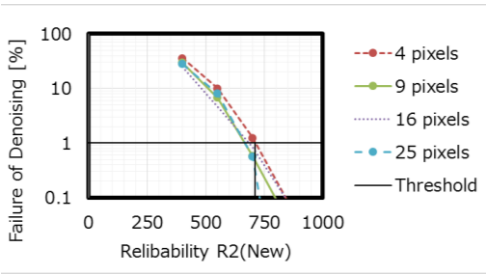

(c) R2 (proposed method 2)

Fig. 4. Relation of Reliability and Failure Rate on De-noising in the sky (success rate 0%)

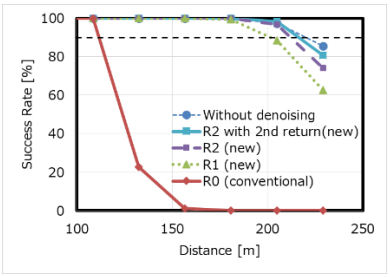

(a) vs. distance (accumulation scope=25)

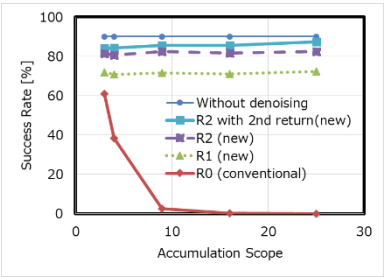

(b) vs. accumulation scope (Decrease due to 99% de-noising)

Fig.5 Success rate

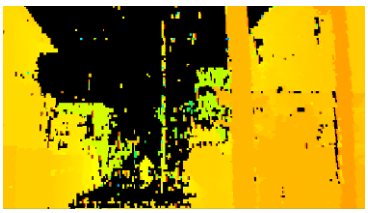

(a) Noise reduction result with R0 (conventional)

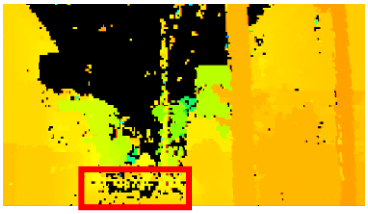

(b) Noise reduction result with R2 (proposed method 2)

Fig.6 Example of range image of a narrow road

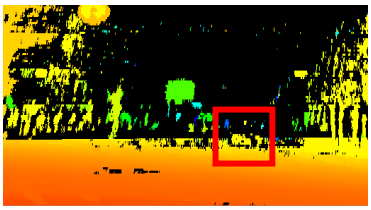

(a) Noise reduction result with R0 (conventional)

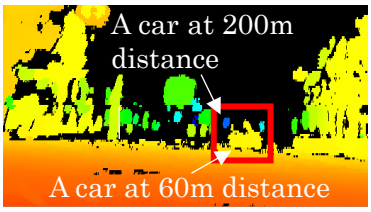

(b) Noise reduction result with R2 (proposed method 2)

Fig.7 Example of range image of cars